Astron. & Astrophys. 33, 289—301 (1974)

The Synthesis Radio Telescope at Westerbork. Principles of Operation, Performance and Data Reduction

J. A. Högbom* and W. N. Brouw
Netherlands Foundation for Radio Astronomy

Received July 31, 1973; revised February 12, 1974

Summary. A description is given of the main properties of the Westerbork Synthesis Radio Telescope as an instrumental system for radio astronomical observations. Sufficient basic aperture synthesis theory is included to derive the main characteristics of the instrument such as the field of view, the synthesized beam, the grating responses, the sidelobe structure and the sensitivity under different operating conditions. The main steps in the standard data processing from the receiver outputs to the computed sky brightness distribution are described as well as some of the commonly used additional programs that are available for the further processing of the maps.

Key words: radio telescope – aperture synthesis – data handling – Fourier transforms

1. Introduction

This paper is one of a series describing the properties and use of the Westerbork Synthesis Radio Telescope (see also Baars and Hooghoudt, 1974; Casse and Muller, 1974; Weiler, 1973; Allen *et al.*, 1974). Here we shall discuss the principles behind the particular type of aperture synthesis employed, the various ways in which the telescope can be used and the available data reduction programs.

The fundamental idea behind aperture synthesis is that a Fourier transform relation exists between the sky radio brightness distribution and the response of a radio interferometer of variable baseline. Thus, the technique of aperture synthesis implies that the observed field of sky must be measured at many different interferometer baselines (Ryle and Hewish, 1960; Ryle, 1962). The Westerbork telescope can be regarded as an assembly of 20 simultaneously operating, but otherwise independent, E – W interferometers: each of the two movable antennas forms an interferometer together with each of the ten fixed antennas (see Table 1).

The length of any interferometer baseline can be altered by shifting one of the two movable antennas to a different position along the railtrack. The orientation of the baseline as seen from a fixed direction in space changes continuously because of the rotation of the Earth; hence, measurements taken at different hour angles are taken at different orientations of the interferometer baseline. Thus the Westerbork array allows measurements to be made at any specified baseline as seen from space up to the projected length of the whole array. A complete "full synthesis" observation, requiring that measurements be taken at all available baseline lengths and orientations, is thus done by measuring a particular piece of sky for 12 hours while the interferometers cover all orientations of the 20 available baselines. Several such 12-h measurements with the movable antennas at different positions along the railtrack are needed to completely cover the full range of spacings. Many observing programs do not require this very time consuming full synthesis and some alternative observing procedures will be discussed in Section 4. The complete set of interferometer measurements is Fourier transformed in a digital computer to produce a radio map or "image" of the piece of sky within the primary beam of the individual antennas (the "field of view").

Table 1. Mechanical data of the Westerbork array (for further details see Baars and Hooghoudt, 1974)

Spacing between the fixed position antennas	144 m
Length of rail for the movable antennas	300 m
Minimum available interferometer spacing	36 m
Maximum available interferometer spacing	1602 m
Diameter of the parabolic reflectors	25 m
Steerable in hour angle	$\pm 6^h$ from the meridian
Steerable in declination	$+90°$ to the horizon
Pointing accuracy in RA[a])	± 0.01 degree
Surface	8 mm mesh, 0.8 mm steel wire
Surface accuracy	1.4 mm rms

[a]) The pointing accuracy in declination has not been quite satisfactory, but steps have been taken to improve the performance.

* Now at Stockholm Observatory

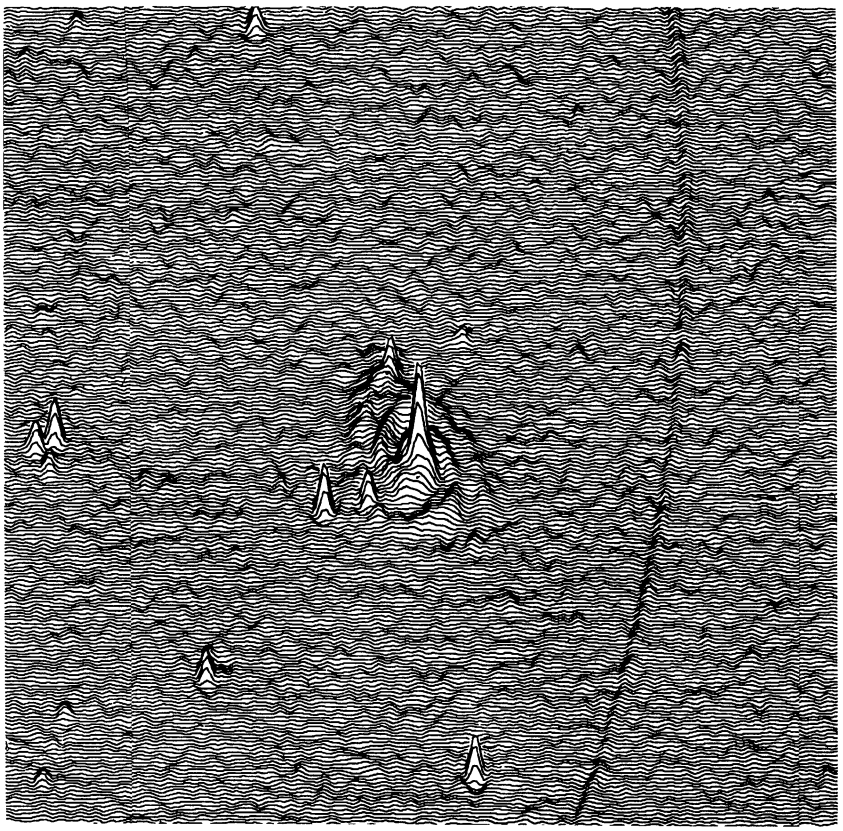

Fig. 1. Part of an image containing the galaxy M 51 based on four 12-h measurements at 1415 MHz (Oort, 1971). The galaxy is a weak radio source and the amplitude scale is such that the noise level ($\simeq 0.5$ mfu rms) is clearly visible over the empty parts of the map. A weak grating ring (see Section 2.4) centered at a source outside the area shown in this map can also be seen

Aperture synthesis telescopes have two main advantages as compared to most other types of radio telescope. First, one can achieve a very high resolving power (a narrow "synthesized beam") for the amount of antenna structure actually built. The angular resolution of the Westerbork maps, for instance, corresponds to the diffraction limited resolving power of a 1600 m diameter filled aperture (sometimes referred to as the "synthesized aperture"). Second, the telescope measures directly a radio image of a complete field rather than the radio brightness in one single direction only. The diameter of the Westerbork image is approximately 100 times that of the synthesized beam and, consequently, a Westerbork map contains information about the sky brightness in some 10^4 independent directions, each of which has been measured over the full observing time (Fig. 1). A single-beam instrument (such as e.g. a Cross-antenna) with the same collecting area and receiver quality must spend the same time on each of these directions separately in order to produce the same map with the same sensitivity. It can of course speed up the procedure and complete all the measurements in the same time as did the synthesis telescope, but then the sensitivity will be a factor $\sqrt{10^4} = 100$ worse because of the reduced integration time per direction.

2. The Westerbork Array as an Aperture Synthesis Instrument

2.1 Basic Aperture Synthesis Relations

The Westerbork array is built along an accurately measured E–W line and all interferometer baselines are at right angles to the Earth's axis of rotation. Any baseline can therefore be specified by the rectangular coordinates (u, v) of the one antenna relative to the other in a plane perpendicular to the Earth's axis[1]) (Fig. 2a). The u and v coordinates are measured in units of one wavelength at the centre frequency of the

[1]) The u, v plane is often defined to be perpendicular to the direction of the observed field centre and a baseline is then specified by its projection onto this plane. However, the projection is not the same seen from directions away from the field centre and this complicates the equations in a way which we avoid by choosing the u, v plane to be that defined by the rotating E–W baselines themselves. The direction ($l=0$, $m=0$) is therefore that of the North Celestial Pole and has no special relation to the observed field. The relation between the coordinates (l, m) and the equatorial coordinates (α, δ) is here:

$l = \sin \Delta\alpha \cdot \cos \delta$

$m = -\cos \Delta\alpha \cdot \cos \delta$

where $\Delta\alpha = \alpha - \alpha_0$ is the right ascension with respect to the field centre. The element of solid angle $d\Omega$ is given by:

$d\Omega = dl\, dm/(1 - l^2 - m^2)^{1/2} = dl\, dm/\sin \delta$.

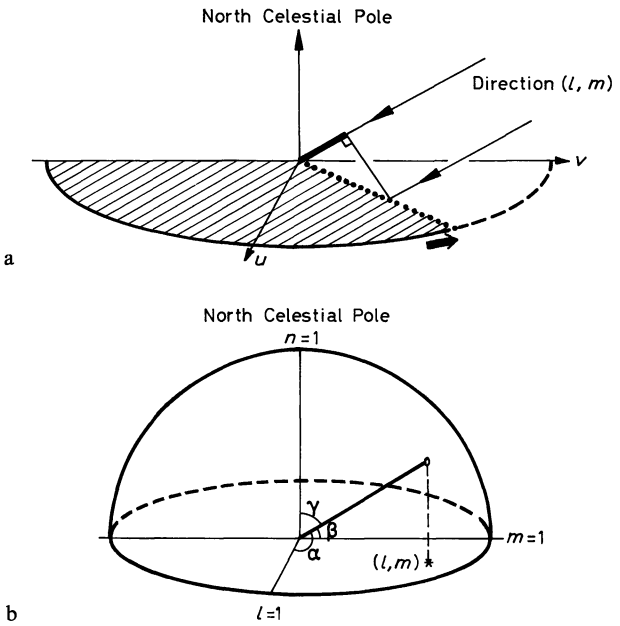

Fig. 2. a The baseline of an E–W interferometer is represented by a point (u, v) in a coordinate system whose axis directions are fixed in space. As the Earth rotates, the 20 interferometers trace out circles with radii equal to their respective baseline lengths in wavelengths. The heavy line marks the difference in path, $(ul+vm)$ wavelengths, between waves from the direction (l, m) striking the two antennas of one interferometer. b A direction in the sky is specified by the directional cosines $l=\cos\alpha$, $m=\cos\beta$ and $n=\cos\gamma$ measured from the $u-$, $v-$ and North Celestial Pole directions respectively. Since l, m, n are related by $l^2+m^2+n^2=1$ it is sufficient to use only the coordinates (l, m), the third coordinate being understood

observed frequency band and the u and v directions are fixed in space. As the Earth rotates, each of the 20 interferometers is represented by a point tracing out a circle centered at the origin and with a radius equal to the baseline length in wavelengths. A direction in the sky is specified by the directional cosines (l, m) with respect to the u and v axis directions, respectively (Fig. 2b).

Consider the radiation from a small solid angle $\Delta\Omega$ in the direction (l, m) falling on an interferometer whose spacing is (u, v). The two antennas receive identical correlated signals except for a difference in the time of arrival of the waves due to the difference in path, $(ul+vm)$ wavelength (Fig. 2). At the band centre frequency this produces a phase difference

$$\psi = 2\pi\,(ul+vm) \quad \text{radians} \tag{1}$$

between the signals from the two antenna outputs. A Westerbork correlation receiver measures the time averages of $a\cdot\cos\psi$ (the cosine output) and $a\cdot\sin\psi$ (the sine output) where the amplitude a is proportional to the correlated output power from the individual antennas. This can be written as a complex receiver output ΔW:

$$\Delta W = a\cdot\cos\psi + i\,a\cdot\sin\psi = a\cdot\exp(i\psi)\,. \tag{2}$$

The correlated power delivered by the individual antennas is proportional to $\Delta\Omega$, to the value of the antenna power pattern P and to the sky brightness temperature T_b. Thus:

$$\Delta W = \text{const}\cdot P\cdot T_b\cdot\Delta\Omega\cdot\exp(i\psi)\,. \tag{3}$$

Integrating this expression over all directions in the sky, we get a full interferometer response to all incoming radiation of

$$W = \text{const}\int_{4\pi} P\cdot T_b\cdot\exp(i\psi)\,d\Omega \tag{4}$$

where P and T_b are functions of the direction (l, m) in the sky. Inserting the value of ψ from Eq. (1) and replacing $d\Omega$ by $dl\,dm/\sin\delta$ gives

$$W(u,v) = \int_{-\infty}^{+\infty}\int\left\{\frac{\text{const}}{\sin\delta}\cdot P\cdot T_b\right\}\exp[i\cdot 2\pi(ul+vm)]\,dl\,dm. \tag{5}$$

Since the integration covers the range $(l^2+m^2)\leqq 1$ which is the whole sky, we can extend our formal limits to $\pm\infty$ and so make the right hand side a Fourier integral. P and T_b are real functions of l and m and we see that

$$W(-u,\,-v) = W^*(u,v) \tag{6}$$

where the star indicates the complex conjugate. Thus, it is sufficient to measure $W(u, v)$ over two adjacent quadrants in the (u, v) plane since the other half of the plane can be determined from Eq. (6). The necessary two quadrants are covered when the antennas continuously track a source for 12 h during which time the Earth rotates the interferometer baselines through 180°.

In this short derivation of the Fourier relation (5) we have ignored several effects of consequence to a working interferometer such as the necessary delay compensation when using a finite receiver bandwidth. For more detailed information in the case of the Westerbork instrument see Brouw (1971) and Casse and Muller (1974). The general theory of radio interferometry and aperture synthesis may be found in Christiansen and Högbom (1969) or Fomalont and Wright (1973).

2.2 Image Formation and Field of View

Inverting the Fourier relation (5) we obtain:

$$\left\{\frac{\text{const}}{\sin\delta}\cdot P\cdot T_b\right\} = \int_{-\infty}^{+\infty}\int W\cdot\exp[-i\,2\pi(ul+vm)]\,du\,dv. \tag{7}$$

Thus, we can calculate the radio brightness distribution $T_b(l, m)$ over the field of view, i.e. the region within the main lobe of the antenna power pattern $P(l, m)$. The $\sin\delta$ factor in the denominator usually varies little over this restricted area of sky. The proportionality constant can in theory be calculated from the antenna

power pattern P and the receiver characteristics, but is best determined from observations of calibration sources with known flux density.

2.3 Synthesized Beam and Grading

It is clearly impossible to make measurements at all spacings (u, v) out to infinity as required by the $\pm\infty$ integration limits of Eq. (7). Thus we will introduce a grading function $g(u, v)$ to weight the measurements $W(u, v)$ before calculating the Fourier transform. The grading $g(u, v)$ is set equal to zero for all spacings (u, v) at which there are no measurements. The product $W(u, v) \cdot g(u, v)$ is thus, in contrast to $W(u, v)$ itself, known for all values (u, v). Replacing W by this product in the integral of Eq. (7) we obtain from the convolution theorem in Fourier analysis

$$\left\{\frac{\text{const}}{\sin\delta} \cdot P \cdot T_b\right\} * G = \iint W \cdot g \cdot \exp\left[-i\,2\pi\,(ul+vm)\right] du\,dv \tag{8}$$

where $G(l, m)$ is the Fourier transform of the grading $g(u, v)$. The symbol $*$ indicates the convolution integral of the expression within the curled brackets and $G(l, m)$. This convolution is equivalent to scanning the field of view with a telescope whose beam has the form $G(l, m)$. Thus this function, normalized to unity at maximum, will be called the synthesized beam. The synthesized beam is therefore proportional to the Fourier transform of the grading $g(u, v)$ whose form we may choose as we desire within the measured area in the (u, v) plane. A uniform grading $(g = 1)$ over this area will result in a beam with a -13% first sidelobe. The sidelobes become smaller, at the expense of a somewhat wider main beam, if the grading function is tapered towards the edges so as to introduce a smoother transition from areas with data to areas without data. The truncated gaussian grading (tapered to 25% at the maximum baseline) normally used in the Westerbork reduction programmes gives a -5% first sidelobe (Fig. 3).

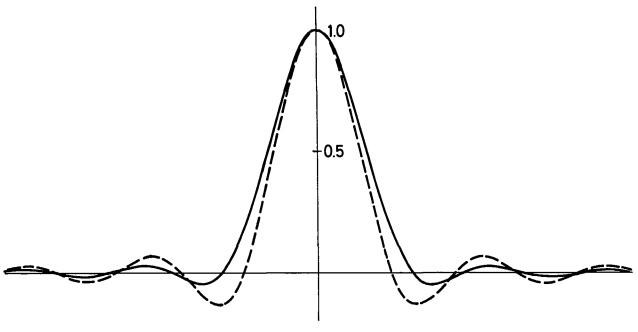

Fig. 3. Cross-section of the synthesized beam for the standard gaussian grading which reaches 0.25 of its maximum value at the largest measured spacing. The dashed curve shows the somewhat narrower beam with larger sidelobes that can be obtained with a uniform grading

The shape of the synthesized beam in the (l, m) coordinate system is independent of the direction in the sky. In angular measure, however, the beam is extended in declination by a factor $1/\sin\delta$. This is obvious also from the fact that the measured (u, v) area is circular only when viewed from the North celestial pole and becomes elliptical in the ratio $1/\sin\delta$ when seen in projection from other declinations. The standard grading results in a synthesized beam whose width between half power points is $0.80/R$ radians in right ascension and $0.80/(R\sin\delta)$ radians in declination where R is the maximum interferometer spacing in wavelengths.

2.4 Grating Responses

During a 12 h observation, the function $W(u, v)$ is only measured along a set of circular tracks in the (u, v) plane. The grading, as defined in the previous section, is equal to zero between these tracks and the smooth gradings discussed above give a simplified impression of the real situation. The finite number of measured tracks results in a synthesized pattern $G(l, m)$ given by the Fourier transform of the true grading, in which central maximum is accompanied by a set of concentric grating circles. Their radii in the (l, m) coordinate system are $k/\Delta r$ where k is an integer and Δr is the regular interval between the measured tracks in wavelengths. Expressed in angular measure these grating circles are ellipses with semi-axes $k/\Delta r$ and $k/(\Delta r \sin\delta)$ radians in the right ascension and declination directions, respectively. The amplitude of a grating ring is inversely proportional to the square root of its radius. Thus, to minimize the disturbances caused by the grating rings, the steps Δr (wavelengths) between the measured circular tracks in the (u, v) plane should be small. A normal 12-h measurement taken with the two movable antennas separated by 72 m (half the

Table 2. Telescope performance data with present receivers after one 12 hour measurement (for further details see Casse and Muller, 1974)

	Frequency MHz		
	610	1415	4995
Antenna aperture efficiency	0.59	0.54	0.44
Antenna half-power beamwidth (field of view)	83′	36′	11′
Synthesized beam, half-power beamwidth (in RA)	56″	24″	6.″8
Radius of closest grating ring (in RA)	23′	10′	2.′8
System noise temperature, K	400	260	200
Receiver equivalent bandwidth, MHz	4.2	4.2	4.2
Sensitivity[a]): $(\Delta S)_{\text{rms}}$, mfu[b])	1.0	0.9	0.9
Sensitivity[a]): $(\Delta T)_{\text{rms}}$, $K/\sin\delta$	1.3	1.2	1.2

[a]) Theoretical values. The fluctuations are generally found to be somewhat higher and to be influenced by the meteorological conditions.

[b]) 1 mfu $= 10^{-29}$ W m^{-2} Hz^{-1}.

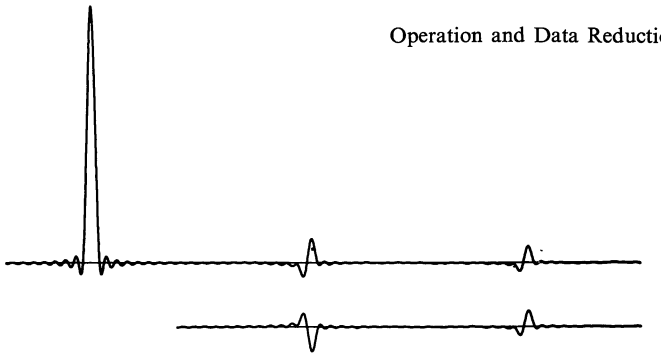

Fig. 4. Cross-section of the synthesized pattern including the closest two grating rings for a single 12 h measurement when the two movable antennas are at 72 and 144 m respectively from the closest antenna of the fixed array. If instead the antennas are placed at 36 and 108 m, the first and all other odd-numbered rings are reversed in amplitude as shown below. Combining the two sets of measurements, one can produce a map corresponding to a synthesized beam in which all the odd numbered grating rings have been eliminated. The remaining rings can be eliminated by making further measurements with the antennas in yet other positions along the rail

spacing between the antennas in the fixed position array) yields values of $W(u, v)$ along a set of concentric circles with regular 72 m spacings (Fig. 2a). This regularity then produces a set of elliptical grating rings whose semi-axes at a wavelength of 21 cm are multiples of 10 arcmin in the right ascension direction and of $10/\sin\delta$ arcmin in the declination direction. The dimensions of the rings, like those of the main synthesized beam are proportional to the wavelength (see Table 2). Figure 4 shows a cross-section of the synthesized pattern including the first two grating rings, and the influence they have on a synthesis map can be seen in Figs. 5 and 6. Adding a second 12-h measurement with the movable antennas shifted by 36 m will give a regular spacing of 36 m between the circles in the (u, v) plane. This corresponds to grating rings with twice the previous radii, i.e. all the odd-numbered rings have been eliminated. After

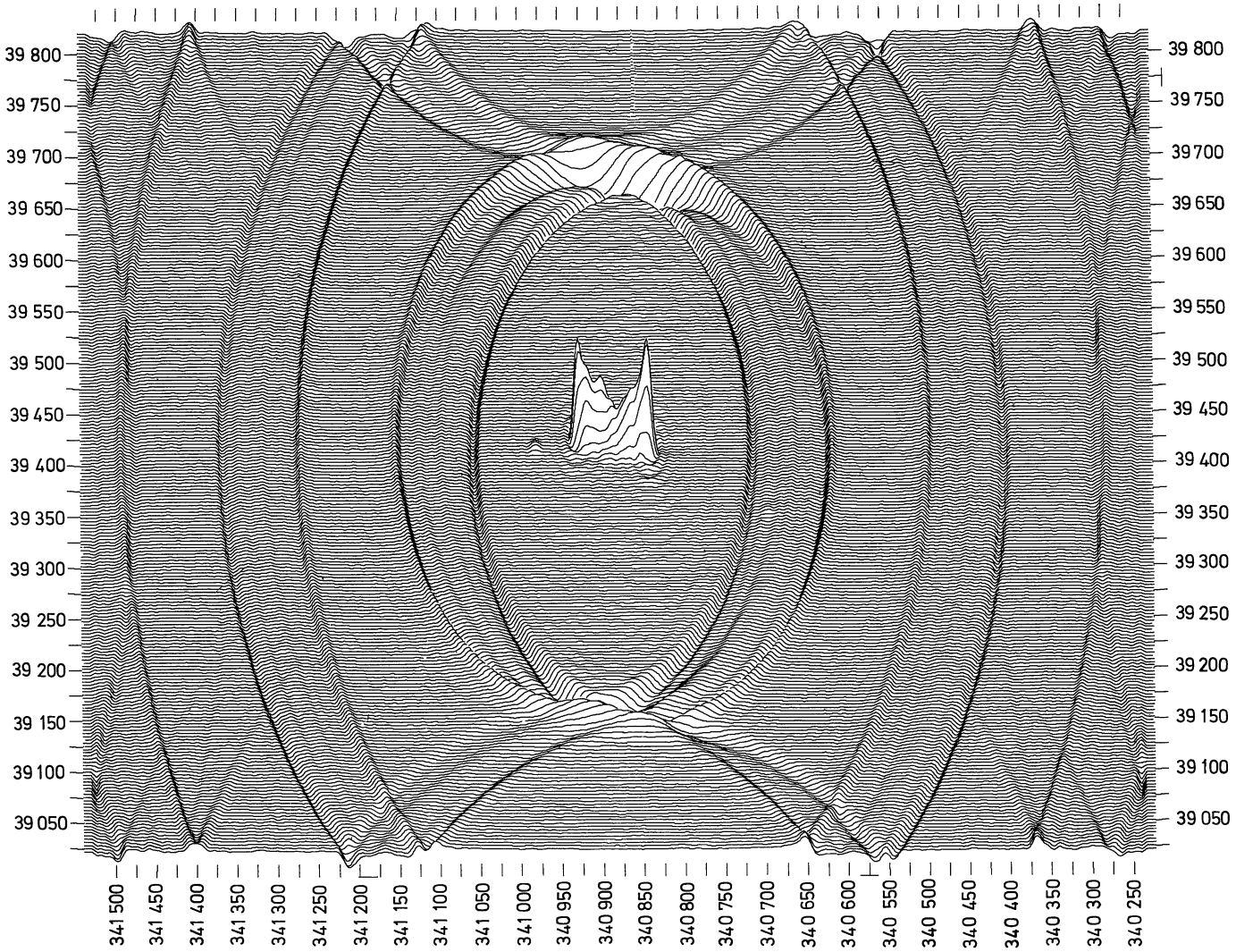

Fig. 5. Profile plot of an image containing the bright radio source 3C452 prepared from a single 12-h measurement at 1415 MHz. Note how the different parts of the source contribute to the confused grating disturbances and that the rings (as well as the main beam) are extended in declination ($\delta = +39°$). The outer parts have been enhanced to compensate for the influence of the primary beam pattern and so make the amplitude scale uniform over the map. Parts of other grating rings centered at the repetition positions of the source outside the map (Section 5.3) can also be seen

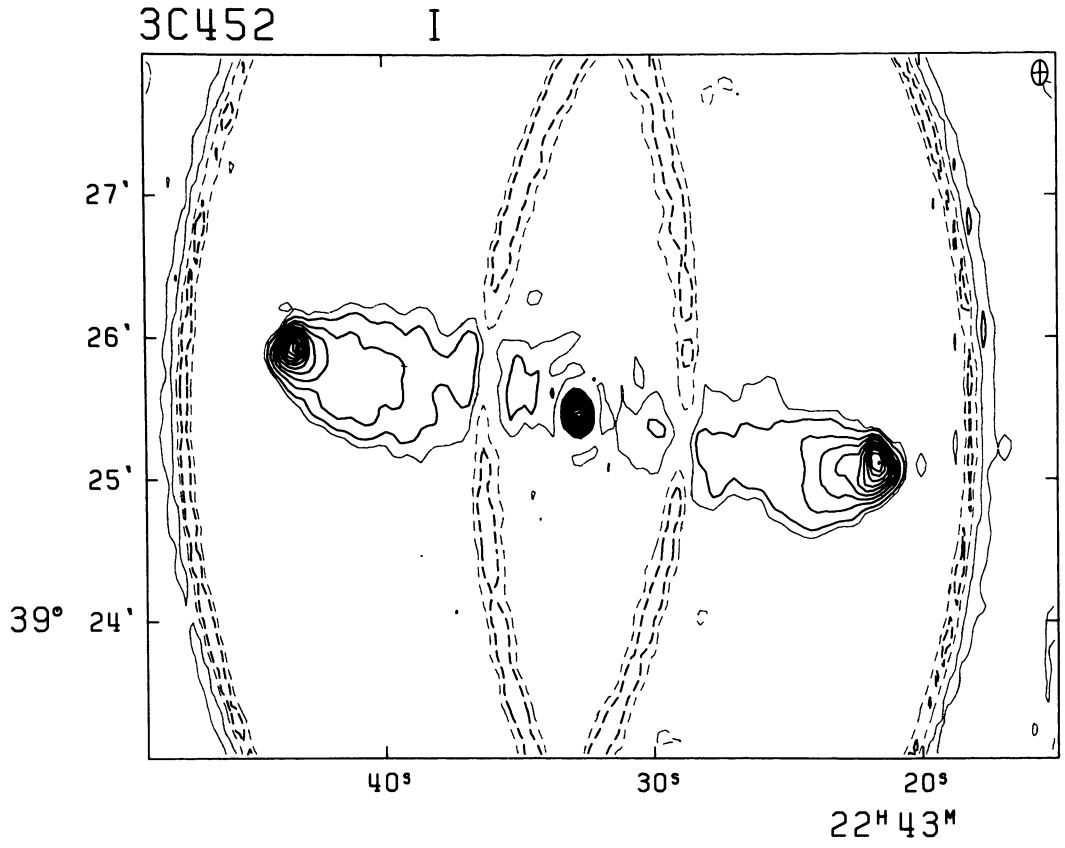

Fig. 6. Contour map of the source 3C452 prepared from a single 12-h measurement at 4995 MHz. Compared with the 1415 MHz map (Fig. 5), the angular resolution here is higher and the grating rings are so close that they disturb the picture of the source. The grating disturbances may be eliminated by special data processing methods or by adding further 12-h measurements with the movable antennas in different positions along the railtrack

2, 4, 8, etc. 12-h measurements with suitable positions of the movable antennas, the remaining grating rings will be 2, 4, 8, etc. times as distant as in the original set of rings. A general treatment of grating rings is given by Bracewell and Thompson (1973).

2.5 Errors, Sidelobes and Confusion

Sidelobes of all kinds will degrade the synthesis map by giving rise to deflections on the map which are not at the position of the source which is their cause. Some sidelobes appear as a consequence of the instrumental design, the choice of observational procedure and missing observations due to equipment malfunction. The detailed shape of these can be calculated exactly. Other sidelobes are caused by atmospheric phase fluctuations and by unavoidable small departures of the instrument from its ideal calibrated performance. These cannot be calculated exactly but it is often possible to estimate their rms amplitude distribution either from measurements or from a knowledge of the general stability of the atmosphere and the critical parts of the instrument.

The set of grating rings discussed in the previous section is an example of the kind of sidelobe structure which can be calculated exactly. The problem of separating source from sidelobe can become serious when, as in Fig. 6, the observed field contains sources which are larger in angular extent than the radius of the first grating ring. In such cases the grating disturbances must be eliminated, either by special data reduction procedures such as CLEAN (Högbom, 1974) or by adding further 12-h measurements.

No good quality measurements can be made at spacings which are smaller than the diameter of the individual antennas (25 m) because then one antenna must be blocking or shadowing part of the aperture of the other. Thus, independent of the number of 12-h observations completed, there will always be a gap of missing short spacings centered at the (u, v) origin. Its radius is a function of the smallest spacing actually used, but will usually be about 30 m. The true grading of the synthesized aperture can therefore be written

$$g(u, v) = g_d(u, v) - g_0(u, v) \qquad (9)$$

where g_d is the desired complete set of circles in the (u, v) plane and g_0 represents those circles close to the origin that have not been measured. The synthesized beam $G(l, m)$ is proportional to the Fourier transform of the grading (Section 2.3) and it follows that:

$$G(l, m) = G_d(l, m) - G_0(l, m) \quad (10)$$

i.e. the true synthesized beam equals the desired beam minus a beam which corresponds to measurements taken only at the missing small spacings. This latter is a broad low amplitude pattern. Thus, the main maximum of the true synthesized beam will be surrounded by an extended low level negative sidelobe structure. The integral over the complete synthesized beam pattern is equal to zero [this is a consequence of $g(0, 0) = 0$] and the integral over a synthesis map must therefore also be zero. The negative sidelobe regions produce a depression of the zero level which varies slowly over the map in a way which depends upon the detailed distribution and intensities of all sources in the field. This does not cause serious problems when studying isolated small diameter sources, because the local zero level is sufficiently well defined by the surrounding empty parts of the map, but one must be very careful when calculating brightness temperatures and integrated flux densities of extended sources (Section 3.3). These problems are avoided if the synthesis measurements are complemented by a survey of the same field taken with a filled aperture telescope whose diameter is larger than the radius of the central gap in the (u, v) plane. The 75 m Jodrell Bank telescope has been used for this purpose in certain cases where extended low level brightness features were vital to the astronomical interpretation of the measurements.

In some observations, notably at low declinations, it is unavoidable that shadowing of one dish by another occurs. In cases where these effects are not too severe, the measured interferometer outputs are corrected for the loss of gain by observationally determined factors. The dynamic range of the telescope is determined by the general sidelobe level caused by those effects – atmospheric fluctuations and instrumental instabilities – which cannot be calculated exactly. A weak source can only be detected if it is well above the random noise level on the map and the general sidelobe interference due to strong sources in the field. At 1415 MHz the individual receiver channels have a phase accuracy of about 2 electrical degrees and a gain stability of a few per cent over a 12 h period. At this frequency, the dynamic range approaches 30 dB over most of the field and it appears that atmospheric phase fluctuations are a major limiting factor at this level (van Someren Greve, 1974).

The term "confusion" is usually employed in radio astronomy to refer to the fact that every observed field contains a large number of weak sources. These cause deflections that merge to a noise-like distribution over the map. For normal synthesis observations with the Westerbork telescope at 1415 MHz (or higher frequencies) this "confusion noise" is below the sensitivity limit and has no influence on the interpretation of the synthesis maps. At lower frequencies, however, the greater flux density of most sources and the larger dimensions of the synthesized beam combine to raise the confusion noise to a level comparable to or greater than the sensitivity limit. The "confusion" problem here is to decide how many deflections on a map can be interpreted as due to individual (point) sources rather than to a blend of many weaker sources. An often stated rule of the thumb is to accept the largest deflections as individual sources but not to count more sources than what corresponds to an average of one source per 20–30 beamwidths. The situation is even more complicated when the beam is accompanied by a prominent sidelobe pattern such as a set of grating rings. The statistical theory of the confusion problem and the influence of the detailed shape of the reception pattern have been discussed by Burns (1972).

2.6 Polarization Synthesis

The output from an interferometer is a function of both the polarization of the incoming radiation and the polarization properties of the instrument itself. Each Westerbork antenna is equipped with a rotatable crossed dipole feed and the two orthogonal dipoles (the "x" and the "y" dipoles) have independent front end equipment. The four possible dipole combinations (xx, xy, yx and yy) of each interferometer are measured simultaneously by independent correlation receiver channels. In this way, the four Stokes parameters can be simultaneously measured and their distributions synthesized. A thorough discussion of polarization synthesis and its application at Westerbork is given by Weiler (1973).

3. Sensitivity and Intensity Scales

3.1 The Definition of Sensitivity

The sensitivity of a radio telescope is usually discussed in terms that suggest that all sources of error in the measurements are caused by random fluctuations with the well-defined statistical properties of thermal noise. This assumption is valid only for ideal observing conditions – no interference, no scintillation and completely stable equipment. In practice, a carefully designed and well built instrument can approach this ideal. The measured performance of the Westerbork telescope is very satisfactory in this respect, especially at night when the meteorological conditions are best.

The sensitivity is a measure of the weakest source which, in the absence of confusing sources, can be

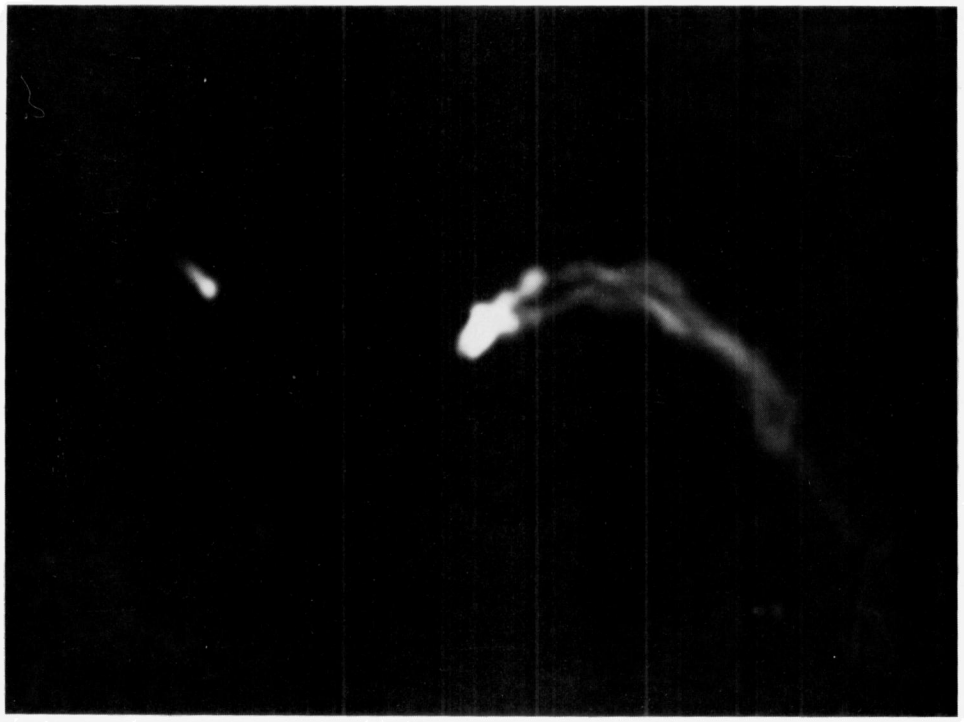

Fig. 7. Radiograph representation of a field containing the radio sources 3C129 and 3C129.1

detected with confidence. It is often defined as the signal corresponding to the rms error deflection σ or as some multiple (usually between 2 and 5) of this number. If, for example, one wishes to determine whether a particular optical object is a radio source, then a positive deflection $\geqq 2\sigma$ at that position may just be considered significant. The probability of a 2σ positive deflection occurring at any one specified position is only about 1/44. If on the other hand one wants to discover previously unknown sources over a whole Westerbork field of view then this factor of 2 is not sufficient: the field of view is 10^4 times larger than the synthesized beam and one expects more than 200 positive deflections $\geqq 2\sigma$ to occur there purely by chance even if the entire field is devoid of radio sources. The same level of confidence (1/44), in this case, can only be achieved by accepting deflections which are $\geqq 4.6\sigma$. The sensitivity for this second program is therefore 2.3 times worse than for the first when the same map with the same rms error is used for both programs. In this section we shall discuss the rms error over the Westerbork image and it should be kept in mind that the sensitivity, that is the minimum deflection that can be considered significant, is larger than this by a factor of between 2 and 5 depending upon the astronomical program.

3.2 The rms *Error in the Measured Flux Density of a Point Source*

The theoretical value of the rms error σ depends upon some factors which are fixed in the overall design of the instrument but also upon the way in which it is being used. The error σ_m in that component of the flux from a point source which is measured by an array of antennas with identically polarized feeds is:

$$\sigma_m = \frac{M}{\eta_s} \frac{k T_{sys}}{(\Delta\nu \cdot t)^{1/2} A_{max} \cdot P\sqrt{N}} \quad \mathrm{Wm^{-2}\,Hz^{-1}} \qquad (11)$$

where:

$k = 1.38 \cdot 10^{-23}\ \mathrm{W\,Hz^{-1}\ degree^{-1}}$, Boltzmann's constant.

T_{sys} = System noise temperature (see Table 2).

$M = 1.6$ factor expressing how much worse the particular receiver is with respect to sensitivity than is an ideal square law detector (see Christiansen and Högbom, 1969). The value is that of a double phase-switch receiver with linear detection and square wave fringe integration.

$\eta_s = 0.9$, factor expressing the loss of sensitivity due to the unequal weights given to the different interferometers by the grading function (Section 2.3). The value of η_s is not very sensitive to the exact shape of the grading.

$\Delta\nu$ = Receiver equivalent frequency bandwidth ($4.2 \cdot 10^6$ Hz with the present continuum receiver backend).

t = Total observing time in seconds, determined by the observing program.

A = Effective (collecting) area of an individual interferometer in the maximum direction. This equals the geometrical area of two 25-metre circular apertures, 982 $\mathrm{m^2}$, multiplied by the aperture efficiency (Table 2).

P = Normalized power pattern of an individual 25 m paraboloid. It is down to a value of 0.5 at about $0.9\,\lambda_{cm}$ arcmin from the maximum direction (Table 2).
$N = 20$, number of simultaneously operating interferometers. (A second pair of movable antennas is planned for 1975; N will then be increased to 40.)
Equation (11) is valid under the assumption that all antennas have identical feeds. The measured flux density S_m as well as the error σ_m will then refer to that component of the incoming radiation whose polarization is "matched" to that of the antennas. The flux density S_c carried in the complementary polarization is not measured. Only if the source is known to be randomly polarized ("unpolarized") can we set the total flux density S equal to twice that measured; the rms error in S is then obviously $2\sigma_m$.
The Westerbork antennas are equipped with crossed dipole feeds and thus the flux density in the two orthogonal polarization directions can be measured independently, each with the same error σ_m given by Eq. (11). The error in $S = S_m + S_c$ will then be given by $\sigma = \sqrt{2} \cdot \sigma_m$. The flux density S is equal to the Stokes parameter I and we mentioned in Section 2.6 that full polarization synthesis (i.e. the determination of the brightness distribution in all four parameters I, Q, U and V) is possible. We state here without proof that the rms error in the determination of each Stokes parameter is the same and equal to that for the parameter I ($\sqrt{2} \cdot \sigma_m$). The error is, in theory, the same for whatever relative position angle settings are used in the two antennas of the individual interferometers. A 45° difference in the feed position angles is normally used at Westerbork (see further Weiler, 1973).
The theoretical rms error in a Westerbork field after an integration time of $4.32 \cdot 10^4$ s (one 12-h period) at 4995 MHz with the present front ends is equal to the expected response to a point source with a flux density

$$(\Delta S)_{rms} = 0.9 \text{ mfu} \quad (1 \text{ mfu} = 10^{-29} \text{ W m}^{-2} \text{ Hz}^{-1})$$

situated at the centre of the field ($P = 1.0$). The corresponding values for the other two frequencies, 610 MHz and 1415 MHz are very similar with the present receivers (Table 2). In practice the rms error is usually found to be somewhat larger than the theoretical value.

3.3 The Relation between the Flux Density and Brightness Temperature Scales on the Map

An extended source with the brightness temperature distribution $T_b(l, m)$ produces, at a position (l_0, m_0) on the map, the same deflection as an isolated point source with the flux density S W m^{-2} Hz^{-1} if

$$S G_{max} = \int_{4\pi} (2k/\lambda^2)\, T_b \cdot G \cdot d\Omega$$

i.e.

$$S = (2k/\lambda^2) \int_{4\pi} T_b \cdot (G/G_{max})\, d\Omega\,. \tag{12}$$

Here $G(l, m)$ represents the shape of the synthesized reception pattern (Section 2.3) with its main maximum centered at (l_0, m_0). The value of the integral is a function of the brightness temperature in all directions where the synthesized pattern is significantly different from zero. If the measured source is alone in the field and relatively small in angular extent, then we can ignore contributions to the integral from grating rings and other sidelobes and write:

$$S \simeq (2k/\lambda^2)\, T_{obs} \int_{c.r.} (G/G_{max})\, d\Omega \tag{13}$$

where T_{obs} is the average source brightness temperature weighted by the central response of the synthesized beam pattern (c.r.). Hence T_{obs} is the value at (l_0, m_0) of the source brightness temperature distribution as observed with the resolution of the Westerbork telescope.
The shape of the synthesized pattern G is the Fourier transform of the grading g (Section 2.3). We shall illustrate the way in which the relation (13) depends upon the choice of $g(u, v)$ by considering a simple "ideal" synthesis in which the measurements are complete for all baselines $(u^2 + v^2) \leqq R^2$. There will then be no extended negative sidelobe and no grating rings and, if the chosen grading is not too extreme, the close sidelobes of the synthesized beam will be negligible beyond some moderate distance from the beam centre. We can then use any convenient integration limits we wish provided they are large enough. The Fourier relation between $G(l, m)$ and $g(u, v)$ implies that:

$$\int_{-\infty}^{+\infty}\int g\, du\, dv = G_{max} \tag{14}$$

and

$$g(0, 0) = \int_{-\infty}^{+\infty}\int G\, dl\, dm = \sin \delta_0 \int_{c.r.} G\, d\Omega \tag{15}$$

where we have approximated sin δ by its value at the centre of the synthesized beam (see footnote on Page 290). Equation (13) can now be written:

$$T_{obs} = S \cdot (\lambda^2/2k) \cdot \sin \delta_0 \iint \frac{g}{g(0, 0)}\, du\, dv \tag{16}$$

or

$$T_{obs} = S \pi k^{-1} R_m^2 \sin \delta_0 \int_0^1 g_r(r)\, r\, dr \tag{17}$$

if, as will normally be the case, the chosen grading has circular symmetry. $g_r(r)$ is the normalized grading in the radial direction ($r = (u^2 + v^2)^{1/2}/R$ and $g_r(0) = 1$) and $R_m = R\lambda$ is the maximum interferometer spacing in metres.
Equation (17) shows that the relation between the brightness temperature and flux density scales depends upon the total length of the array, the grading and the declination but is independent of the frequency. At Westerbork with $R_m \simeq 1440$ m (the two movable antennas in the commonly used configuration 72 and

144 m from the closest fixed antenna), a 1 mfu point source should produce the same deflection on the map as does an extended region whose brightness temperature is

$$\begin{aligned} T_b &= 2.4 \sin \delta_0 \,(K) \quad \text{(uniform grading)} \\ T_b &= 1.3 \sin \delta_0 \,(K) \quad \text{(standard truncated gaussian grading)}. \end{aligned} \tag{18}$$

The declination dependence reflects the fact that the equivalent solid angle of the synthesized beam is a function of the declination.

Usually, an observed field contains more than one simple source so that one should, if possible: a) make enough 12-h observations to eliminate the influence of grating rings (Section 2.4) and b) obtain the missing small spacing information (Section 2.5) for example from a survey of the field made with a large parabolic reflector telescope. This is especially important when observing sources which extend over large portions of the field.

If such precautions are taken or if the observed source is small in angular measure both compared with the radius of the first grating ring and the solid angle occupied by the negative sidelobe caused by the missing small spacing measurements, then Eq. (17) can be used to find the brightness temperature distribution of the source.

3.4 Sensitivity to Extended Objects at Different Angular Resolutions

The relation between the rms error on the map expressed in flux density units and in brightness temperature units is of course also governed by Eq. (17). The rms flux density error after one 12-h measurement (with the present receivers, see Table 2) that has been reduced with the standard truncated gaussian grading will thus correspond to an error $(\Delta T_b)_{\rm rms}$ of about $1.2 \sin \delta$ (K).

The sensitivity to weak extended sources can be improved by smoothing the map to correspond to observations which have been made with a wider synthesized beam. From simple considerations one might expect an improvement by a factor $(\Omega_w/\Omega_0)^{1/2}$ where Ω_w and Ω_0 are the solid angles of the widened and the original beam respectively, but the Westerbork maps in fact show a greater improvement. The source fine structure which is eliminated by the smoothing is due to the measured values of $W(u, v)$ at the larger spacings in the (u, v) plane. These values are known with relatively low accuracy because the interferometers here scan along their circles at greater speeds. Consequently, the smoothing procedure systematically eliminates the less accurate measurements and thus improves the sensitivity over the expected factor given above.

If the smoothing widens the synthesized beam in both dimensions by a factor q we are, in effect, using only the measurements from an array $1/q$ times as long. The number of interferometers N in Eq. (11) and the maximum baseline R_m in Eq. (17) are then both reduced by the factor q. The result is that $(\Delta S)_{\rm rms}$ increases by a factor $q^{1/2}$ but $(\Delta T_b)_{\rm rms}$ decreases by $q^{3/2}$. A factor of two improvement in the sensitivity to extended sources can thus be achieved either by observing four times as long or by smoothing the map to correspond to one measured with a beam which is a factor $2^{2/3} = 1.6$ wider in both dimensions.

4. Standard Observing Procedures

4.1 Calibration Measurements

To obtain accurate source positions, the baseline parameters of the synthesis array must be known. The line on which the antennas are placed was carefully surveyed by geodetic and astrometric means to an accuracy of about 1 mm in relative position, and about 2″ in geographic longitude and azimuth (see Baars and Hooghoudt, 1974). However, the coordinate system to which all Westerbork measurements are referred is based on radio measurements of optically identified small diameter sources. This is inherently more accurate than the geodetic and astrometric optical measurements because they cannot take into account the small differences between the mechanical and electrical properties of the individual antennas.

A consistent set of optical positions of radio sources is available from Murray *et al.* (1969), and a selection of these sources are observed regularly to determine the parameters and check the stability of the telescope. At 1415 MHz the stability has been found to be approximately 2% in gain and 2 electrical degrees in phase over a period of one week.

4.2 Measurements Occupying One or More 12-h *Periods*

A 12-h measurement in which the observed region of sky is followed in hour angle from $-6^{\rm h}$ to $+6^{\rm h}$ is the basic mode of operation for 2-dimensional synthesis and the type of measurement for which the telescope was specifically designed. One single 12-h measurement is sufficient to produce a map of the whole field with full angular resolution in both dimensions. However, all sources in the image are accompanied by a set of concentric grating rings. Several 12-h measurements taken with the two movable antennas at different positions along the rail track can be combined to give a map in which the grating rings are weaker and at greater distances from the source. After 4 periods ("full synthesis"), the piece of sky observed can be mapped with virtually no disturbances caused by these grating effects (Section 2.4).

The "full synthesis" procedure will clearly produce maps of the highest possible quality, but it is extremely time-consuming and should be resorted to only when absolutely necessary. Well-defined individual point sources can, if desired, be subtracted from the map together with their sidelobes and grating rings (see Section 5.3) and the presence in the field of a few prominent sources is in itself no reason for taking more than one 12-h measurement. On the other hand, an image that contains large areas with a complex radio structure can only be mapped satisfactorily with the full synthesis procedure. Several 12-h measurements may also be necessary if the program requires higher sensitivity. One must, however, consider whether an increase in the observing time from 12 h to $n \cdot 12$ h is a reasonable price to pay for a $\sqrt{n}$ improvement in the sensitivity. When observing weak extended sources, one can, for instance, achieve the same improvement in the sensitivity by preparing the map with a resolution that corresponds to a $\sqrt[3]{n}$ times wider synthesized beam (Section 3.4).

4.3 Short Observations

The term "short observation" is used to describe a measurement that requires less than one hour to complete. This somewhat arbitrary definition derives from the way in which different types of observing program are scheduled on the telescope.

During a short observation the baseline will rotate only a fraction of the 180° which are required for normal two-dimensional synthesis and, disregarding some minor effects caused by the finite rotation, one obtains a strip scan through the radio sources in the observed field. Grating responses, whose shapes depend upon the relative size of the smallest spacing r_1 and the regular baseline step Δr, occur at distances corresponding to the baseline step Δr and at the position angle perpendicular to the projected baseline. Compared with a complete 12-h observation the short observation has the following main characteristics:

1) Good resolution is achieved only in the direction parallel to the projected baseline of the array (i.e. a strip scan of the field is produced).

2) The sensitivity with respect to point sources will be 2–10 times worse than that of a complete 12-h period because of the reduced integration time t [Eq. (11)]. The sensitivity to extended objects however, is less affected because the large solid angle of the synthesized fan beam partly compensates for the shorter integration time.

3) The much larger solid angle of the synthesized fan beam has the effect that confusion problems (Section 2.5) become more severe.

4) The short measurement is much more economical with respect to telescope time and should be chosen whenever a complete two-dimensional synthesis is not absolutely necessary.

Two short measurements taken at different hour angles will be sufficient to define the positions in both coordinates of the more prominent sources in a field; one additional measurement would make it possible also to determine diameters and position angles of simple extended sources. A set of short observations of a not too complex field can be processed by the procedure CLEAN (Högbom, 1974) to yield a two-dimensional brightness distribution approaching that of a full synthesis observation in quality.

5. Data Reduction

5.1 General Principles

The synthesis telescope receivers measure the Fourier transform of the sky brightness distribution. The most direct way to arrive at the desired brightness distribution itself would be by way of some analogue processing device. Attempts have been made to build analogue systems for this type of problem (see e.g. McLean *et al.*, 1967) but the practical difficulties seem to be very great indeed. It is also difficult to imagine an analogue device that will be flexible enough to admit a wide range of standard (and non-standard) modes of operation. Thus, the present data reduction package has been based entirely on processing by a digital computer.

The basic design of the various data reduction programs has been described by Brouw (1971) and van Someren Greve (1974). A series of stenciled manuals (Brouw *et al.*, 1969–1974) give details about the input and output requirements and options, controlcard format etc., and a "WSRT Observers Handbook" (Weiler *et al.*, 1972) contains practical information including examples of controlcards for different purposes.

Both the overall design and the details of the data processing package have been made as modular as possible, each module having its specific task. Changes in the receiver system, the calibration procedures or the astronomical applications can then easily be incorporated either by modifying an already existing module or by adding a new module designed for the new task to be performed. Each large module is a separate computer program, which accepts as input the output of another program plus some control information. It produces an output that goes either to the astronomer, or to a following program module.

The program package can be split into the following classes:

I.	Data collection	(on-line computer).
II.	Data correction	(off-line computer).
III.	System calibration	(off-line computer).
IV.	Fourier transform	(off-line computer).
V.	Astronomical application	(off-line computer).

5.2 On-line Data Handling at Westerbork (I)

The data collection program is part of the general program package for the on-line computer at Westerbork. (It also controls antenna steering, fringe-stop and delay-line switching and a number of other functions during an observation.) The 160 outputs from the 80 complex correlator channels (20 interferometers with 4 polarization channels) are read at intervals of 10 s. The sum of the last three readings for all outputs are written on a magnetic tape at intervals of 30 s together with information about the behaviour of the receiving system and some administrative data.

Plans for extending the on-line computing facilities at Westerbork are well advanced. Once this extension has been implemented, the data correction and most of the error finding will be performed in real-time at the observatory (Raimond, 1974). The programs MAKEOBS and MAKECAL (cf. Section 5.3) will then be carried out simultaneously with the observations.

5.3 Routine Off-line Data Processing (II–IV)

Most of the further data reduction is at present performed by the IBM 370/158 computer at the Leiden University computing centre. The Westerbork tapes are here read by the correction program (MAKEOBS), which corrects the raw measurements for refraction, precession, nutation and aberration as well as for the known instrumental errors. It then writes the corrected measurements in a rearranged and compressed form on a second tape. Error messages are printed when the program encounters inconsistencies in the measurements or in the administrative data (e.g. telescope pointing). The program itself takes action to eliminate or reduce the effects of a number of minor troubles such as missing measurements, bursts of interference, etc.

The calibration program (MAKECAL) accepts as input the output tapes of the correction program for calibration sources. The observed objects should ideally be strong unpolarized point sources of accurately known position and intensity. The program calculates the (X, Y, Z)-positions of all the twelve telescopes relative to a reference east-west line and determines the gain and collimation error for each individual complex receiver channel. The results are printed and also punched on cards to be used as control cards for the MAKEOBS reductions of the observed fields.

The Fourier transform program (MAKEMAP) accepts the output tape from MAKEOBS and produces a map of the radio brightness distribution over any specified part of the observed field. Sources with known positions can be subtracted from the measurements before the Fourier inversion if desired. This is valuable if one is interested in weak components in the presence of a strong source.

The program is also used to compute the expected synthesized beam, i.e. the response of the instrument to an ideal point source if all instrumental errors were perfectly known and had been corrected for. The Westerbork telescope has proved to be very stable and the differences between the expected and the real beam patterns are generally very small. These differences may, however, become significant when one attempts to remove a very strong source from a map by the subtraction procedure described above.

The fast Fourier transform algorithm is used, which means that the measurements, which lie on concentric circles in the (u, v) plane, must first be transformed to a rectangular grid. The values on these grid points are obtained by convolving the measured points with a gaussian function, and computing the values of this convolution at the desired grid points. This convolution procedure in effect multiplies the map by another gaussian function which is the Fourier transform of the convolving function. The program corrects the transform for this effect before delivering the final map. A minor disadvantage of this technique is that the Fourier transform of a set of values on a rectangular grid is repetitive. This can result in extra grating rings centered at the repetition positions of a source outside the computed map (Fig. 5). Similarly, sources which are in fact situated outside the map area may appear inside this area. These effects will not cause any serious problems if the map is computed for a large enough area. A source outside the map must then, in effect, also be outside the main beam of the individual antennas and its influence will be correspondingly reduced.

5.4 Astronomical Application Programs (V)

This general title covers a variety of programs whose tasks are to present the information on the output tape from the Fourier transform program in a form that is suitable for the further astronomical interpretation. Some of the more commonly used programs are described below.

COMBI Produces a new map from two or more input maps. The program can be used to produce maps of polarization intensities or position angles, integrated hydrogen line flux, mean radial velocities etc.

SRTPLOT Draws profiles of the sky brightness at equal intervals in declination (or in right ascension) as a function of the other direction variable. The result is a picture in the form illustrated in Figs. 1 and 5. The program can also be used to plot single profiles at specified position angles through a given point on the map.

CONTOUR Draws lines connecting points of equal amplitude on the map (Fig. 6). Any desired set of contour intervals may be specified.

PLOTPOL Plots a map of vectors representing the intensity and the position angle of the linearly polarized radiation.

SEARCH Searches any specified region of the map for sources and delivers a table of the positions and flux densities of the detected sources. It can also be used to determine the exact map position of a source whose approximate position is known.

OVERLAY Searches either the AGK $2(-2° < \delta < +90°)$ or the YALE $(-31° < \delta < -2°)$ catalogues for standard stars within about 1 degree of an input field centre. The positions of these stars are plotted on the scale of the standard Palomar Sky Survey prints. A printed listing is produced of the catalogue numbers and positions of the plotted stars.

SRTPHOTO Produces an intensity modulated display on an oscilloscope screen, which can be photographed so as to produce a representation a "radiograph" which is analogous to that of normal optical photographs (Fig. 7).

INTERACTIVE A set of programs which allow the user to perform various operations on a synthesis map and observe the effect of each step on a cathode ray oscilloscope screen. The available operations include coordinate transformations, source analysis, removal of grating and other sidelobe disturbances by the process CLEAN (Högbom, 1974), combination of different maps, etc.

Acknowledgement. It is a pleasure to thank Dr. K. W. Weiler for his interest and constructive criticism which has led to many improvements in the presentation of the material.

The Westerbork Radio Observatory is operated by the Netherlands Foundation for Radio Astronomy with the financial support of the Netherlands Organization for the Advancement of Pure Research (Z.W.O.).

References

Allen, R.J., Hamaker, J.P., Wellington, K.J. 1974, *Astron. & Astrophys.* **31**, 71
Baars, J.W.M., Hooghoudt, B.G. 1974, *Astron. & Astrophys.* **31**, 323
Bracewell, R.N., Thompson, A.R. 1973, *Astrophys. J.* **182**, 77
Brouw, W.N. 1971, Thesis University of Leiden
Brouw, W.N. *et al.* 1969–1974, stenciled manuals for using the Westerbork data reduction programs, available to observers working with the Synthesis Radio Telescope
Burns, W.R. 1972, *Astron. & Astrophys.* **19**, 41
Casse, J.L., Muller, C.A. 1974, *Astron. & Astrophys.* **31**, 333
Christiansen, W.N., Högbom, J.A. 1969, Radiotelescopes, Cambridge, University Press
Fomalont, E.B., Wright, M.C.H. 1973, in *Galactic and Extragalactic Radio Astronomy*, Ed., G. L. Verschuur and K. I. Kellermann, Springer-Verlag (in press)
Högbom, J.A. 1974, *Astron. & Astrophys. Suppl.* **15**, 417
McLean, D.J., Lambert, L.B., Arm, M., Stark, H. 1967, *Proc. IREE Australia* **28**, 375
Murray, C.A., Tucker, R.H., Clements, E.D. 1969, *Nature* **221**, 1229
Oort, J.H. 1971, Netherlands Organization for the Advancement of Pure Research (ZWO), Yearbook 1970
Raimond, E. 1974, *Astron. & Astrophys. Suppl.* **15**, 525
Ryle, M. 1962, *Nature* **194**, 517
Ryle, M., Hewish, A. 1960, *Monthly Notices Roy. Astron. Soc.* **120**, 220
Someren Greve, H.W. van 1974, *Astron. & Astrophys. Suppl.* **15**, 343
Weiler, K.W. 1973, *Astron. & Astrophys.* **26**, 403
Weiler, K.W., Wolderingh, J.J.H., van den Akker, P. 1972, WSRT Observers Handbook, available to observers working with the Synthesis Radio Telescope

J. A. Högbom
Stockholms Observatorium
S–133 00 Saltsjöbaden, Sweden

W. N. Brouw
Sterrewacht
Leiden–2401, The Netherlands